Neutrosophic-based correlation analysis for fingerprint image pattern recognition and matching

Vinoth D and Ezhilmaran Devarasan*

School of Advanced Sciences, Vellore Institute of Technology, Vellore.

vinov002@gmail.com;   *ezhil.devarasan@yahoo.com

Abstract. A sophisticated mathematical model known as neurosophic extends the vague concept to tackle real-world issues and applications. The neutrosophic connection of the image can be harnessed to ascertain its correlation pattern. This paper aims to employ the neutrosophic method for detecting correlations among fingerprint images using neutrosophic-based pattern analysis. Additionally, it will propose four strategies for identifying relationships within image data by employing the neutrosophic approach. The study explores the four fundamental forms of fingerprint images and experiments with various α values. An α value of 0.99 or higher is favored for image matching.

Keywords: Neutrosophic computer vision; neutrosophic image processing; neutrosophic correlation; fingerprint image matching; neutrosophic biometric

1. Introduction

About Biometric. Biometric is a human recognition system that refers to characteristics of their biological and behavioral. The types of biometrics are facial recognition, fingerprints, finger geometry, iris recognition, vein recognition, retina scanning, voice recognition, DNA matching, and digital signatures. Generally, biometric recognition contains two steps which are enrollment and recognition. First, the system captures the person's physiognomy to create a digital representation, and it becomes a template to be compared by the enrollment systems. The recognition system distinguishes the person's characteristics converting this into the same digital format as the template. Fingerprint identification is based on the analysis of the ridge patterns on the tips of fingers. Sensors generate images of the ridges, and these were scanned their for structural features (called minutiae) such as branches or terminations [10].

Origin of Neutrosophic. The fuzzy concept was first introduced by Zadeh [11] which deals with membership functions, and this concept solves real life problems successfully. The Fuzzy Logic

System (FLS) was first implemented in pattern recognition by Mendel [14]. Zimmermann evaluates the efficiency of fuzzy concepts in computer vision [31] , Atanassov [1] proposed the Intuitionistic Fuzzy Sets (IFS) in 1986 the extension of IFS is known as Neutrosophic Set (NS) is a advanced mathematical concept and also a branch of philosophy which was introduced by Smarandache [23] in 1998 which discuss about membership function (T), non-membership function (F), indeterminacy membership function (I). The correlation for neutrosophic data initially originated from Hanafy et al., [9]. Later the correlation coefficient for interval neutrosophic set formulated by Broumi et al [32]. Image matching measures the degree of similarity between two image sets that are superimposed on one another plays an important role in many areas, such as pattern recognition, image analysis, and computer vision [29]. The similarity was measured by various operations: feature extraction, distance transformation, and similarity measurement.

This article, section 1 gives a brief introduction about fuzzy sets and neutrosophic sets. Then, section 2 focuses on the related work based on image processing and image similarities with the concept of fuzzy sets and neutrosophic sets. The following section 3 defines some basic definitions of neutrosophic sets for the image domain. Then, section 4 explains our contribution in this article to find the relationship between the images. The experimental analysis is done in section 5, here we do three types of analysis methods. Methodology-1 finds the relationship between the two images. Methodology-2 is based on relationship finding the matching for multiple images. To calculate the performance quality of proposal methodology-3 experiments with a combined image database. Finally, section 6 gives the conclusion of the proposal based on the getting results.

2. Related work

I.K.Vlachos [27] used the Intuitionistic fuzzy cross-entropy and discrimination approach to determine distance, similarity, dissimilarity, and correlation. This allows us to obtain image discrimination information. Guo, et al. [6] find neutrosophic similarity scores this approach can find two different criteria which are the local mean intensity criterion and local homogeneity of the images. R.M.Zulqarnain, et al. [32] used the Multipolar interval-valued neutrosophic soft set (mPIVNSS) method to find the similarity measurement in medical diagnoses. In this proposal, Euclidean distance and Hamming distance are used for finding the similarity distances. Gao Q. [7] invented a comparison of fake and real fingerprint images based on different types of sensors. The author used the NIST database and ATVS-FFp database for analysis. This proposal distinguished between authentic and fake fingerprint images using the matching score. Jun Ye [28] introduced simplified neutrosophic sets (SNSs) for Cosine similarity measurements. This method is very useful in medical image diagnosis problems.

M.Baskar, et al. [2] introduced Region Centric Minutiae Propagation Measure (RCMPM) which removes noise from the image based on a forgery detection algorithm and classifies the minutiae, loop, whorl is some basic patterns to classify the fingerprint images. R.P.Sharma, and S.Dey [21] used together Fuzzy c-means technique, Gabor filter, Fourier transforms, and a diffusion filter to extract classification features such as mean, moisture, variance, uniformity, contrast, ridge valley area uniformity, and ridge valley for the fingerprint images. Two-stage quality adaptive fingerprint image enhancement method can classify the images as the classes dry, wet, normally dry, normal wet, and good [30]. The identification of gender also relied on fingerprints. Based on fingerprints, Gustisyaf et al. [8] classified gender using a convolutional neural network. The classification accuracy value for 49270 images is 99.9667%. For the SDUMLA-HMT database, gender determination is achieved with 99.8% accuracy [17] which used feature-level fusion. The Linear Discriminant Analysis, K-Nearest Neighbor classifier, and Support Vector Machine algorithms were addressed in this proposal. The accuracy for the KNN correlation method was 89.8%. Narwal et al. [16] proposed an algorithm that is not restricted to the local fingerprint image features, such as a ridge, location, and direction. In order to select the best principal features, the author used the PCA algorithm. The Gabour filter made it much smoother to match the templates.

3. Preliminaries

Definition 3.1. Let A be an universe of data, the element in A denoted by a, then the neutrosophic set (NS), of the object A is in the form $[3, 22]$

$$A = \{(a, T_A(a), I_A(a), F_A(a)\}$$

where the neutrosophic membership functions $T, I, F : A \to]^-0, 1^+[$ define respectively the degrees of truth, indeterminacy and the falsity of the element $a \in A$ to the set condition.

$$^-0 \leq T_A(a) + I_A(a) + F_A(a) \leq 3^+$$

Definition 3.2. A neutrosophic image P_{NS} is charecterized with neutrosophic membership functions which are T, I, F where P_{NS} are the intensities of the image. Universally for neutrosophic image approach is gray intensities of the image. The image neutrosophic set is defined as $[3, 5]$

$$P_{NS}A(i, j) = \{T_A(i, j), I_A(i, j), F_A(i, j)\} \tag{1}$$

In general the arithmetic mean is consider as truth membership values and the standard deviation of the image is consider as indeterminacy membership. The neutrosophic transformation

intensity of the image is define by the following formulae

$$
\begin{aligned}
T_A(i,j) &= \frac{\bar{p}(i,j) - \bar{p}\min}{\bar{p}\max - \bar{p}\min} \\
\bar{p}_A(i,j) &= \frac{1}{w*w} \sum_{m=i-\frac{w}{2}}^{m=i+\frac{w}{2}} \sum_{n=j-\frac{w}{2}}^{n=j+\frac{w}{2}} p(m,n) \\
I_A(i,j) &= \frac{\delta(i,j) - \delta\min}{\delta\max - \delta\min} \\
\delta_A(i,j) &= abs(p(i,j) - \bar{p}_A(i,j)) \\
F_A(i,j) &= 1 - T_A(i,j)
\end{aligned}
$$

where $\bar{p}_A(i,j)$ denotes the pixel mean in the region $w*w$ and w is generally $w = 2n+1, \ (n \geq 1)$.

4. Proposed method

Definition 4.1 (Neutrosophic correlaltion). Let $A = [a_{i,j}]_{m \times n}$ and $B = [b_{i,j}]_{m \times n}$ be two images with m rows and n columns then the image's neutrosophic correlation is defined as follows

$$
K(A,B) = \frac{\frac{1}{3}C(A,B)}{\delta_A \delta_B} \tag{2}
$$

where

$$
\begin{aligned}
C(A,B) &= \left(\begin{pmatrix} \max(T_A(i \pm \Delta i, j \pm \Delta j), T_B(i \pm \Delta i, j \pm \Delta j)) - \\ \max(I_A(i \pm \Delta i, j \pm \Delta j), I_B(i \pm \Delta i, j \pm \Delta j)) + \\ \max(F_A(i \pm \Delta i, j \pm \Delta j), F_B(i \pm \Delta i, j \pm \Delta j)) \end{pmatrix} \right) \\
\delta(A_{ij}) &= \frac{1}{3} \sqrt{T_A(i,j)^2 + I_A(i,j)^2 + F_A(i,j)^2} \\
\delta(B_{ij}) &= \frac{1}{3} \sqrt{T_B(i,j)^2 + I_B(i,j)^2 + F_B(i,j)^2}
\end{aligned}
$$

Then the correlation pattern for the matching level value α is defined as

$$
\Im[K(A,B)]_{m \times n} = \begin{cases} K(A,B) & \text{if } K(A,B) \geq \alpha \\ 0 & \text{otherwise} \end{cases} \tag{3}
$$

If we need to find the correlation pattern for the image B then

$$
{}_B\Im[K(A,B)]_{m \times n} = \begin{cases} b_{ij} & \text{if } \Im[K(A,B)] = K(A,B) \\ 0 & \text{otherwise} \end{cases} \tag{4}
$$

Definition 4.2 (Neutrosophic Based Spearman Rank correlation). Let $A = [a_{i,j}]_{m \times n}$ and $B = [b_{i,j}]_{m \times n}$ be two images with m rows and n columns. Let $A's$ truth membership subset $T[a(i, i \pm \Delta i, j, j \pm \Delta j)$ contains $X_{T_i} = (x_{T_1}, x_{T_2}...x_{T_n})$ data and $B's$ truth membership subset $T[b(i, i \pm \Delta i, j, j \pm \Delta j)$ contains $Y_{T_i} = (y_{T_1}, y_{T_2}...y_{T_n})$ data. The image's neutrosophic

based Spearman Rank correlation is defined as follows

The truth membership's correlation is

$$r_T(a_{ij}, b_{ij}) = \frac{\sum_{i=1}^{n}(r(X_{T_i}) - \overline{r(X_T)}).(r(Y_{T_i}) - \overline{r(Y_T)})}{\sqrt{[\sum_{i=1}^{n}(r(X_{T_i}) - \overline{r(X_T)})^2][\sum_{i=1}^{n}(r(Y_{T_i}) - \overline{r(Y_T)})^2]}} \tag{5}$$

where

$$
\begin{aligned}
r(X_{T_i}) &= \text{rank of } X_{T_i} \\
r(Y_{T_i}) &= \text{rank of } Y_{T_i} \\
\overline{r(X_T)} &= \frac{\sum_{i=1}^{n} r(X_{T_i})}{N} \\
\overline{r(Y_T)} &= \frac{\sum_{i=1}^{n} r(Y_{T_i})}{N} \\
N &= \text{Total number of the data}
\end{aligned}
$$

Similarly, indeterminacy rank correlation is

$$r_I(a_{ij}, b_{ij}) = \frac{\sum_{i=1}^{n}(r(X_{I_i}) - \overline{r(X_I)}).(r(Y_{I_i}) - \overline{r(Y_I)})}{\sqrt{[\sum_{i=1}^{n}(r(X_{I_i}) - \overline{r(X_I)})^2][\sum_{i=1}^{n}(r(Y_{I_i}) - \overline{r(Y_I)})^2]}}$$

Then the neutrosophic based Spearman Rank correlation of universal image data is

$$r_{NR}(A, B)_{m \times n} = \max\{P((r_T(a_{ij}, b_{ij})_{m \times n}), P(r_I(a_{ij}), b_{ij})_{m \times n})\}$$

For the correlation pattern matching value of α then the image is as follows

$$_{\alpha}r_{NR}(A, B)_{m \times n} = \begin{cases} r_{NR}(A, B) & \text{if } r_{NR}(A, B) > \alpha \\ 0 & \text{if } r_{NR}(A, B) \le \alpha \end{cases} \tag{6}$$

The image B's correlation pattern is

$$\Im(_{\alpha B}r_{NR}(A, B)_{m \times n}) = \begin{cases} b_{ij} & \text{if } _{\alpha}r_{NR}(A, B) > \alpha \\ 0 & \text{if } _{\alpha}r_{NR}(A, B) \le \alpha \end{cases} \tag{7}$$

Definition 4.3 (Neutrosophic Based Kendall Rank Correlation). Let $A = [a_{i,j}]_{m \times n}$ and $B = [b_{i,j}]_{m \times n}$ be two images with m rows and n columns. Let $A's$ truth membership subset $T[a(i, i \pm \Delta i, j, j \pm \Delta j)$ contains $X_{T_i} = (x_{T_1}, x_{T_2}...x_{T_n})$ data and $B's$ truth membership subset $T[b(i, i \pm \Delta i, j, j \pm \Delta j)$ contains $Y_{T_i} = (y_{T_1}, y_{T_2}...y_{T_n})$ data. The image's neutrosophic based Kendall Rank correlation is defined as follows

The truth membership's correlation is

$$\tau_T(a_{ij}, b_{ij}) = \frac{\sum_1^n \sum_1^n sign(X_{T_{ki}} - X_{T_{kj}})sign(Y_{T_{ki}} - Y_{T_{kj}})}{n(n-1)}$$

The indeterminacy membership rank correlation is

$$\tau_I(a_{ij}, b_{ij}) = \frac{\sum_1^n \sum_1^n sign(X_{I_{ki}} - X_{I_{kj}})sign(Y_{I_{ki}} - Y_{I_{kj}})}{n(n-1)}$$

Then the neutrosophic based Kendall rank correlation for global image data is

$$\tau_{NR}(A, B)_{m \times n} = \{\max(P(\tau_{T(a_{ij}, b_{ij})})), \max(P(\tau_{I(a_{ij}, b_{ij})}))\}$$

For the correlation pattern matching value of α then the image is as follows

$$_\alpha\tau_{NR}(A, B)_{m \times n} = \begin{cases} \tau_{NR}(A, B) & \text{if } \tau_{NR}(A, B) > \alpha \\ 0 & \text{if } \tau_{NR}(A, B) \le \alpha \end{cases} \tag{8}$$

The image B's correlation pattern is

$$\Im(_{\alpha B}\tau_{NR}(A, B)_{m \times n}) = \begin{cases} b_{ij} & \text{if } _\alpha\tau_{NR}(A, B) > \alpha \\ 0 & \text{if } _\alpha\tau_{NR}(A, B) \le \alpha \end{cases} \tag{9}$$

Definition 4.4 (Neutrosophic Based Karl Pearson Correlation). Let $A = [a_{i,j}]_{m \times n}$ and $B = [b_{i,j}]_{m \times n}$ be two images with m rows and n columns. Let $A's$ truth membership subset $T[a(i, i \pm \Delta i, j, j \pm \Delta j)]$ contains $X_{T_i} = (x_{T_1}, x_{T_2}...x_{T_n})$ data and $B's$ truth membership subset $T[b(i, i \pm \Delta i, j, j \pm \Delta j) \text{ contains } Y_{T_i} = (y_{T_1}, y_{T_2}...y_{T_n})]$ data. The image's neutrosophic based Karl Pearson correlation is defined as follows

The truth membership's rank correlation is

$$\rho_T(a_{ij}, b_{ij}) = \frac{\sum_{i=1}^{n}(X_{T_k} - \overline{X_{T_k}})(Y_{T_k} - \overline{Y_{T_k}})}{\sqrt{\sum_{i=1}^{n}(X_{T_k} - \overline{X_{T_k}})^2}\sqrt{\sum_{i=1}^{n}(Y_{T_k} - \overline{Y_{T_k}})^2}}$$

The indeterminacy membership rank correlation is

$$\rho_I(a_{ij}, b_{ij}) = \frac{\sum_{i=1}^{n}(X_{I_k} - \overline{X_{I_k}})(Y_{I_k} - \overline{Y_{I_k}})}{\sqrt{\sum_{i=1}^{n}(X_{I_k} - \overline{X_{I_k}})^2}\sqrt{\sum_{i=1}^{n}(Y_{I_k} - \overline{Y_{I_k}})^2}}$$

Then the neutrosophic based Karl pearson correlation for global image data is

$$\rho_{NR}(A, B)_{m \times n} = \max\{P(\rho_T(a_{ij}, b_{ij})_{m \times n}), P(\rho_I(a_{ij}, b_{ij})_{m \times n})\}$$

For the correlation pattern matching value of α then the image is as follows

$$_\alpha\rho_{NR}(A, B)_{m \times n} = \begin{cases} \rho_{NR}(A, B) & \text{if } \rho_{NR}(A, B) > \alpha \\ 0 & \text{if } \rho_{NR}(A, B) \le \alpha \end{cases} \tag{10}$$

The image B 's correlation pattern is

$$\Im(_{\alpha B}\rho_{NR}(A, B)_{m \times n}) = \begin{cases} b_{ij} & \text{if } _\alpha\rho_{NR}(A, B) > \alpha \\ 0 & \text{if } _\alpha\rho_{NR}(A, B) \le \alpha \end{cases} \tag{11}$$

Algorithm 1 The correlation pattern

Require: T, I, F values of Image A & B

   for $i = 1 : m, j = 1 : n$ **do**

      $c_1 = \Im[K(A, B)]_{m \times n}$

      $c_2 =_\alpha \tau_{NR}(A, B)_{m \times n}$

      $c_3 =_\alpha r_{NR}(A, B)_{m \times n}$

      $c_4 =_\alpha \rho_{NR}(A, B)_{m \times n}$

      if mean$(c_1 + c_2 + c_3 + c_4 < \alpha)$ **then**

         Output (correlation pattern exist)

      else if mean$(c_1 + c_2 + c_3 + c_4 \geq \alpha)$ **then**

         Output (matching pattern exist)

      end if

   end for
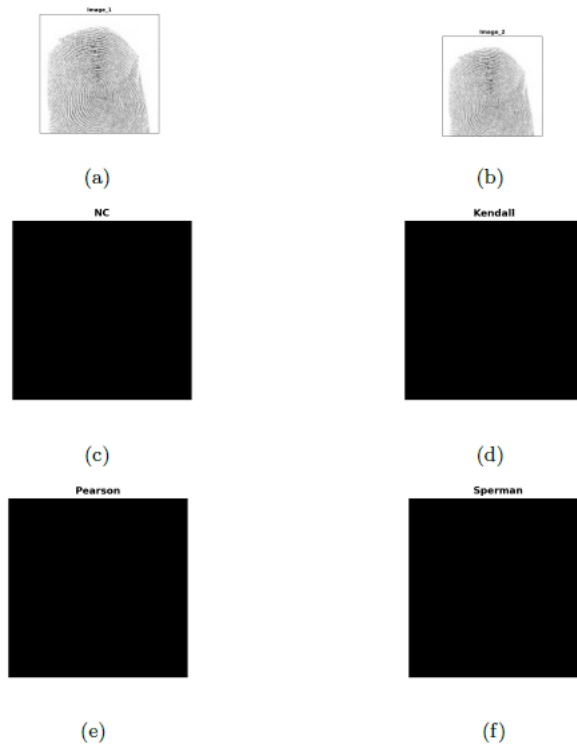
FIGURE 1. Proposed methods output for similar images. $\alpha = 0.9$, $h = 3$

5. Experiments and discussions

Finding the image's relationship is performed in the image matching task. Here we took fingerprint images as our application. The fingerprint image data is collected by the National Institute of Standards and Technology (NIST) database [4] named as SD302 which was organized by the Inteligence Advanced Research Projects Activity (IARPA), in September 2017.
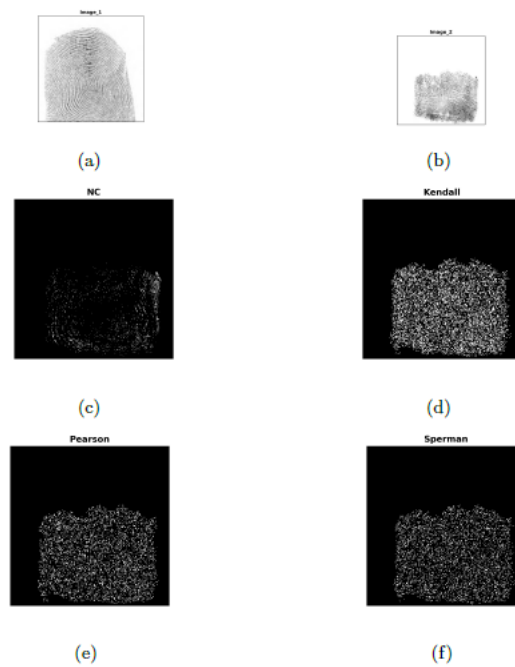
FIGURE 2. Proposed methods output for non-similar images. $\alpha= 0.9$, $h= 3$

Initially, the information pertaining to each latent fingerprint image was obtained by isolating the enclosed section from a comprehensive scene capture. The bounding coordinates were of non-rectangular shape, and pixels beyond this confined region were white. The dimensions of the image were approximated to be 1000 pixels per inch in terms of width and height. NIST supplied the image in Portable Network Graphics (PNG) format to facilitate utilization within conventional image processing software.

Arches: The finger's ridges form an uninterrupted pattern from end to end without any backward turns. Generally, an arch doesn't have a delta, but if it does, there shouldn't be a curving ridge between the core and delta points.

Loops: Loops involve ridges that make a backward turn without twisting. The loop's direction on the hand, rather than the card used for impressions, characterizes this backward rotation. The fingerprint impression resembles a mirror's reverse image. A loop pattern typically has only one delta.

Whorls: In a whorl pattern, at least one set of ridges forms a circuit. Therefore, any pattern with two or more deltas is classified as a whorl.

Tented arch: Similar to the plain arch, the tented arch pattern starts on one side of the finger and flows consistently to the other side.

The sample visualization of similar image is shown in Figure 1. We can determine that there are no patterns between the images because of their similarity. The α value in this case is fixed at 0.9. We get a matching score of 0.99 on average for images that are similar. We can deduce
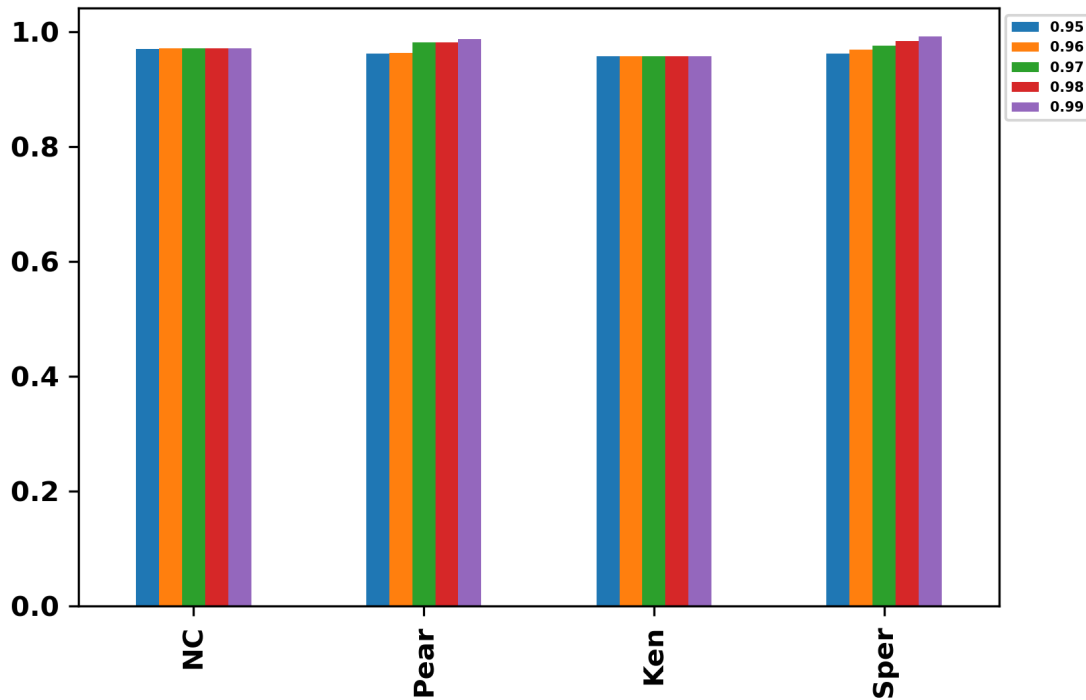
FIGURE 3. Analysis for multiple α values

that there is a perfect match between the images if the average matching score is 0.99 or higher. Whether the images are the same or not can be determined with clarity in this way. When the images are not similar to one another, Figure 2 illustrates the correlation between the images. The proposed approach reaches each type correlation pattern for non-similar images. Different variations exist for each method's matching score. We can determine the correlation pattern level of the images cumulatively based on the average matching score. When there are no similarities between the images, the proposed methods assist us in identifying correlation patterns.

The α factor is used in the next analysis. Our first task is to adjust the α value for better correlation patterns. We are able to obtain each correlation pattern and matching score for every α value. Therefore, the better α values must be fixed. Figure 3 illustrates the matching score level for the non-similar images. Here, we focus on values between 0.95 and 0.99. The NC, Pearson, Kendall, and Spearman methods exhibit the best matching score for the similar pictures for the taken values when $\alpha = 0.99$. If the images have the same patterns, this method of analysis helps us find the matching; otherwise, when the images have different patterns, we can experience correlation patterns. The matching score for each type of image is listed in Table 1 below. According to the table, perfect matching images have an average matching
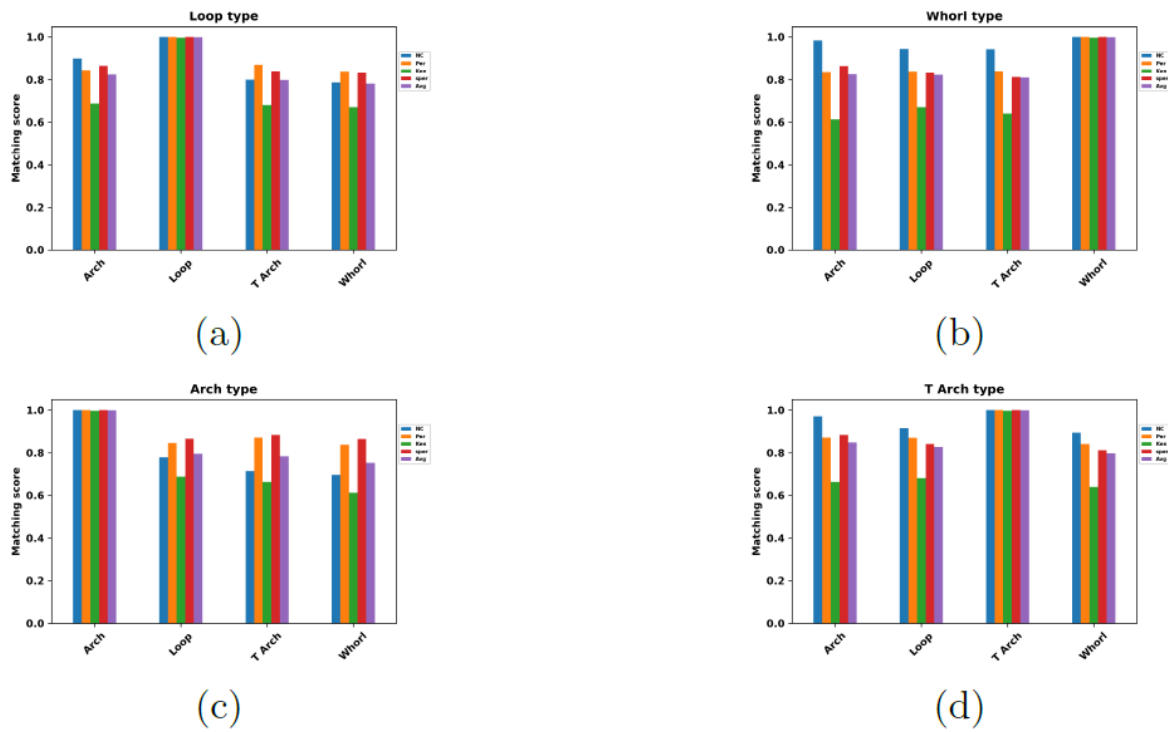
FIGURE 4. Fingerprint image type matching score analysis. (a) loop, (b) whorl, (c) arch, (d) tented arch
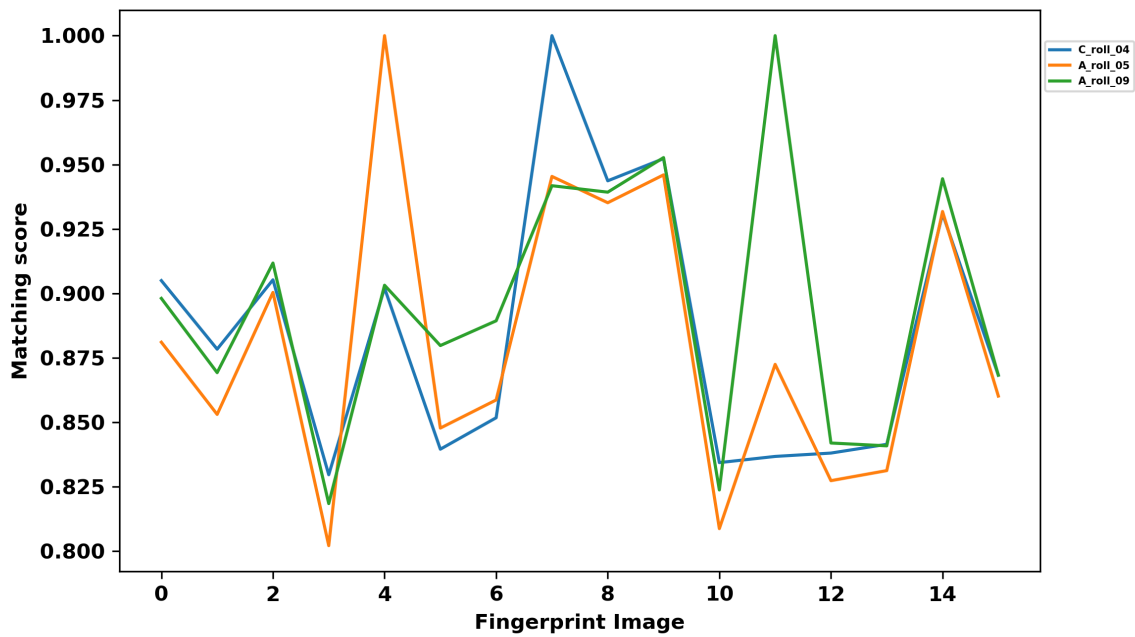
FIGURE 5. Result of random images

TABLE 1. Fingerprint type wise analysis

Image Type	NC	Pearson	Kendall	Spearman	Average
Loop	0.8976	0.8464	0.688	0.8656	0.8244
	1	1	0.9968	1	0.9992
	0.8	0.8704	0.6816	0.8416	0.7984
	0.7872	0.84	0.672	0.832	0.7828
Whorl	0.984	0.8384	0.6128	0.864	0.8248
	0.9456	0.84	0.672	0.832	0.8224
	0.944	0.8416	0.64	0.8128	0.8096
	1	1	0.9968	1	0.9992
Arch	1	1	0.9968	1	0.9992
	0.7792	0.8464	0.688	0.8656	0.7948
	0.7136	0.872	0.664	0.8848	0.7836
	0.696	0.8384	0.6128	0.864	0.7528
T Arch	0.9712	0.872	0.664	0.8848	0.848
	0.9152	0.8704	0.6816	0.8416	0.8272
	1	1	0.9968	1	0.9992
	0.8944	0.8416	0.64	0.8128	0.7972

score greater than 0.99, indicating that the images were similar. If not, there are differences between the images. From the previous analysis we obtain the best matching score alpha should be greater or equal to 0.99 and the h is should be 3.

Based on these values we will analysis the further analysis. We choose two random images from each SD302 dataset types for the final analysis. Since we have already captured, the images could be any kind of fingerprint image. The image's dimensions are fixed at 250 by 250. $h = 3$, $\alpha = 0.99$. We selected three images at random from the generated dataset. Since we used three sample images for matching, the average matching score for the remaining three images was below 0.99. This means that the alpha value for those three images should be greater than 0.99. The data set includes plain, rolled, and touch-free impression fingerprints as well as numerous sets of plain palm impressions that were taken from a variety of devices. All these types were chosen by the article under analysis for analysis. The results of the proposed methods matching scores are listed in Table 2. From the table, we observed that only three images the random image attained the highest level of matching score. This proves how well the proposed technique worked with both similar and dissimilar images. Additionally found the accurate matching for images chosen at random. This demonstrates the method's duality.

TABLE 2. Proposed methods result for random image matching

Random image ID		
C_roll_04	**A_roll_05**	**A_roll_09**
0.905 ± 0.0764	0.8811 ± 0.0288	0.8981 ± 0.0195
0.8784 ± 0.1085	0.8531 ± 0.0642	0.8693 ± 0.022
0.9053 ± 0.0902	0.9004 ± 0.0291	0.9118 ± 0.0294
0.8297 ± 0.1706	0.8022 ± 0.1155	0.8185 ± 0.0599
0.9021 ± 0.0731	1.0 ± 0.0	0.9032 ± 0.0653
0.8396 ± 0.1595	0.8478 ± 0.0692	0.8798 ± 0.0376
0.8518 ± 0.1524	0.8587 ± 0.047	0.8894 ± 0.0466
1.0 ± 0.0	0.9454 ± 0.0126	0.9418 ± 0.0271
0.9437 ± 0.0251	0.9352 ± 0.0186	0.9393 ± 0.032
0.9523 ± 0.0268	0.946 ± 0.0155	0.9527 ± 0.0268
0.8344 ± 0.162	0.8088 ± 0.1126	0.8238 ± 0.0609
0.8368 ± 0.1617	0.8725 ± 0.035	1.0 ± 0.0
0.8381 ± 0.1475	0.8274 ± 0.0734	0.842 ± 0.0447
0.8415 ± 0.1445	0.8313 ± 0.0677	0.8409 ± 0.0436
0.9309 ± 0.0609	0.9318 ± 0.0249	0.9445 ± 0.0332

6. **Conclusion**

We proposed four different types of correlation methods based on neutrosophic sets in this article. We have performed analysis for a number of fingerprint image types, including the arch, loop, whorl, and tented arch. According to the analysis, it is very hard to identify the matching between the images without first fixing the matching pattern. Therefore, we tried to look at the matching task for different α values. Finally, an α value of 0.99 results in better image matching patterns. The findings suggest that there is matching if the matching score is greater than or equal to the α . If it is less, we can recognise the image's correlation patterns. We can perform the matching task locally for the fingerprint images since it went well. We will expand the concept in the feature to include gradient-level image matching.

References

1. Atanassov, K. T., & Stoeva, S. (1986). Intuitionistic fuzzy sets. Fuzzy sets and Systems, 20(1), 87-96.

2. Baskar, M., Renuka Devi, R., Ramkumar, J., Kalyanasundaram, P., Suchithra, M., & Amutha, B. (2023). Region centric minutiae propagation measure orient forgery detection with finger print analysis in health care systems. Neural Processing Letters, 55(1), 19-31.

3. Dhatchinamoorthy, V., & Devarasan, E. (2023). An Analysis of Global and Adaptive Thresholding for Biometric Images Based on Neutrosophic Overset and Underset Approaches. Symmetry, 15(5), 1102. `https://doi.org/10.3390/sym15051102`

4. Fiumara, G. P., Flanagan, P. A., Grantham, J. D., Ko, K., Marshall, K., Schwarz, M., ... & Boehnen, C. (2019). Nist special database 302: Nail to nail fingerprint challenge.

5. Guo, Y., Cheng, H. D., & Zhang, Y. (2009). A new neutrosophic approach to image denoising. New Mathematics and Natural Computation, 5(03), 653-662.

6. Guo, Y., Şengür, A., & Ye, J. (2014). A novel image thresholding algorithm based on neutrosophic similarity score. Measurement, 58, 175-186.

7. Gao, Q. (2014). A Preliminary Study of Fake Fingerprints. International Journal of Computer Network & Information Security, 6(12).

8. Gustisyaf, A. I., & Sinaga, A. (2021). Implementation of Convolutional Neural Network to Classification Gender based on Fingerprint. International Journal of Modern Education & Computer Science, 13(4).

9. Hanafy, I. M., Salama, A. A., & Mahfouz, K. (2012). Correlation of neutrosophic Data. International Refereed Journal of Engineering and Science (IRJES), 1(2), 39-43.

10. Heyer, R. (2008). Biometrics technology review 2008. DSTO.

11. Klir, G. J., & Yuan, B. (Eds.). (1996). Fuzzy sets, fuzzy logic, and fuzzy systems: selected papers by Lotfi A Zadeh (Vol. 6). World Scientific.

12. Lee, S., & Jeong, I. R. (2021). Improved fingerprint indexing based on extended triangulation. IEEE Access, 9, 8471-8478.

13. Lu, Z., & Ye, J. (2017). Cosine measures of neutrosophic cubic sets for multiple attribute decision-making. Symmetry, 9(7), 121.

14. Mendel, J. M. (1995). Fuzzy logic systems for engineering: a tutorial. Proceedings of the IEEE, 83(3), 345-377.

15. Miyazawa, K., Ito, K., Aoki, T., Kobayashi, K., & Nakajima, H. (2008). An effective approach for iris recognition using phase-based image matching. IEEE transactions on pattern analysis and machine intelligence, 30(10), 1741-1756.

16. Narwal, S., & Kaur, D. (2016). Comparison between minutiae based and pattern based algorithm of fingerprint image. International Journal of Information Engineering and Electronic Business, 8(2), 23.

17. Patil, A., Kruthi, R., & Gornale, S. (2019). Analysis of multi-modal biometrics system for gender classification using face, iris and fingerprint images. International Journal of Image, Graphics and Signal Processing, 11(5), 34.

18. Pratamasunu, G. Q. O., & Farisi, O. I. R. (2021). A Neutrosophic Approach to Edge Detection Using Ant Colony Optimization. International Journal on Electrical Engineering & Informatics, 13(3).

19. Ren, H., Xiao, S., & Zhou, H. (2019). A chi-square distance-based similarity measure of single-valued neutrosophic set and applications. Infinite Study.

20. Riaz, M., & Hashmi, M. R. (2021). M-polar neutrosophic soft mapping with application to multiple personality disorder and its associated mental disorders. Artificial Intelligence Review, 54, 2717-2763.

21. Sharma, R. P., & Dey, S. (2019). Two-stage quality adaptive fingerprint image enhancement using Fuzzy C-means clustering based fingerprint quality analysis. Image and Vision Computing, 83, 1-16.

22. Smarandache, F. (1998). Neutrosophy: neutrosophic probability, set, and logic: analytic synthesis & synthetic analysis.

23. Smarandache, F. (1999). A unifying field in logics. neutrosophy: Neutrosophic probability, set and logic.

24. Song, S., Jia, Z., Yang, J., & Kasabov, N. K. (2020). A fast image segmentation algorithm based on saliency map and neutrosophic set theory. IEEE Photonics Journal, 12(5), 1-16.

25. Vlachos, I. K., & Sergiadis, G. D. (2007). Intuitionistic fuzzy information–applications to pattern recognition. Pattern recognition letters, 28(2), 197-206.

26. Wang, L., Chen, B., Xu, P., Ren, H., Fang, X., & Wan, S. (2020). Geometry consistency aware confidence evaluation for feature matching. Image and Vision Computing, 103, 103984.

27. Xu, Z., Chen, J., & Wu, J. (2008). Clustering algorithm for intuitionistic fuzzy sets. Information sciences, 178(19), 3775-3790.

28. Ye, J. (2015). Improved cosine similarity measures of simplified neutrosophic sets for medical diagnoses. Artificial intelligence in medicine, 63(3), 171-179.

29. You, J., & Bhattacharya, P. (2000). A wavelet-based coarse-to-fine image matching scheme in a parallel virtual machine environment. IEEE Transactions on image processing, 9(9), 1547-1559.

30. Yun, E. K., & Cho, S. B. (2006). Adaptive fingerprint image enhancement with fingerprint image quality analysis. Image and Vision Computing, 24(1), 101-110.

31. Zimmermann, H. J. (2011). Fuzzy set theory—and its applications. Springer Science & Business Media.

32. Zulqarnain, R. M., Siddique, I., Asif, M., Ahmad, S., Broumi, S., & Ayaz, S. (2021). Similarity measure for m-polar interval valued neutrosophic soft set with application for medical diagnoses. Neutrosophic Sets and Systems, 47(1), 11.